

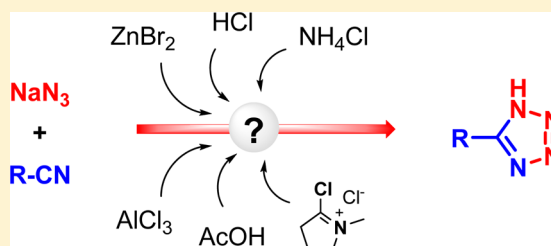
An Experimental and Computational Assessment of Acid-Catalyzed Azide-Nitrile Cycloadditions

David Cantillo, Bernhard Gutmann, and C. Oliver Kappe*

Christian Doppler Laboratory for Microwave Chemistry (CDLMC) and Institute of Chemistry, Karl-Franzens-University Graz, Heinrichstrasse 28, A-8010 Graz, Austria

S Supporting Information

ABSTRACT: The mechanism of the azide–nitrile cycloaddition mediated by different Brønsted and Lewis acids has been addressed through DFT calculations. In all cases activation of the nitrile substrate by the Brønsted or Lewis acid catalyst was found to be responsible for the rate enhancement. According to DFT calculations the cycloaddition proceeds in a stepwise fashion involving the initial formation of an open-chain imidoyl azide intermediate. Kinetic experiments performed using *N*-methyl-2-pyrrolidone as solvent and sodium azide as azide source demonstrate that all evaluated Brønsted acids have the same efficiency toward cycloaddition with benzonitrile, suggesting that hydrazoic acid is the actual dominant catalytic species in these tetrazole syntheses. Lewis acids such as Zn or Al salts perform in a similar manner, activating the nitrile moiety and leading to an open-chain intermediate that subsequently cyclizes to produce the tetrazole nucleus. The most efficient catalyst evaluated was 5-azido-1-methyl-3,4-dihydro-2*H*-pyrrolium azide, which can readily be generated in situ from aluminum chloride, sodium azide in *N*-methyl-2-pyrrolidone. The efficiency of this catalyst has been examined by preparation of a series of 5-substituted-1*H*-tetrazoles. The desired tetrazole structures were obtained in high yields within 3–10 min employing controlled microwave heating.



INTRODUCTION

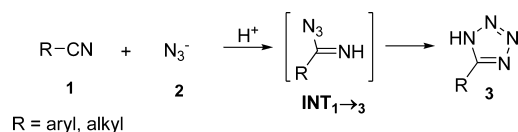
Tetrazole-containing molecules have numerous applications in a wide variety of fields, including organic synthesis, coordination chemistry, material science, and medicinal chemistry.^{1,2} Most notably, 5-substituted tetrazoles are frequently used as surrogates for carboxylic acids in pharmaceutically active agents as they offer similar physicochemical properties, but higher lipophilicities and better metabolic resistance.² Not surprisingly, therefore, a large number of synthetic protocols for the synthesis of tetrazole derivatives were reported in the past decades, and several recent review articles survey their manifold applications in medicinal chemistry and methods of preparation.²

Different strategies for the synthesis of 5-substituted tetrazoles do exist, but by far the most common approach is the Huisgen addition of the azide anion to the nitrile in the presence of an acid catalyst (Scheme 1).^{1,2} The addition of hydrazoic acid to the cyanide group was first observed in 1901 by Hantzsch and Vagt, who prepared 5-aminotetrazole from

hydrazoic acid and cyanamide.³ The parent heterocycle was synthesized by Dimroth and Fester in 1910 by the addition of hydrazoic acid (HN₃) to hydrocyanic acid.⁴ The authors suggested that an imidoyl azide is formed as an intermediate, which then rapidly cyclizes to form the tetrazole. The preparation of 5-alkyl- and 5-aryl-tetrazoles by the addition of hydrazoic acid to alkyl and aryl nitriles was finally accomplished in 1950 by Mihina and Herbst.⁵ Today, hydrazoic acid is hardly used as a reagent in organic synthesis due to its volatility (the boiling point is 37 °C), its high toxicity (comparable to that of HCN), and its dangerously explosive character. It is therefore generally preferred to use inorganic azide salts in combination with a suitable acid as catalyst.⁶ In the majority of cases sodium azide is used as the azide source, and a broad variety of acidic catalysts, ranging from soluble Brønsted^{7,8} or Lewis acids^{9–11} to various heterogeneous¹² and nanocrystalline¹³ catalysts, have been employed to accelerate the azide–nitrile addition.

As mentioned above, the early pioneers of tetrazole synthesis contemplated a stepwise mechanism for the tetrazole formation, where an imidoyl azide is initially formed and subsequently cyclizes to the tetrazole moiety.^{4,5} In recent years, however, it became clear that reactions of a dipolarophile with a 1,3-dipolar structure are generally concerted [2_s + 4_s] cycloadditions, similar to Diels–Alder reactions. Mechanistic studies with a B3LYP density functional theory method

Scheme 1. Acid-Catalyzed Synthesis of 5-Substituted-1*H*-tetrazoles from Nitriles and Azide Salts



Received: October 15, 2012

Published: November 5, 2012

performed in the groups of Sharpless and Noodleman in 2002 and 2003^{14,15} and related investigations performed in our group in 2011¹⁶ indicated that the uncatalyzed reaction of an azide with a nitrile is indeed a concerted asynchronous 1,3-dipolar cycloaddition. In the presence of a proton, however, the reaction appears to proceed via a protonated imidoyl azide as an intermediate (INT₁₋₃, Scheme 1). In this case, the azide ion reveals its nature as a powerful nucleophile and attacks the electron-poor carbon atom of the activated nitrile before the nitrogen–nitrogen bond starts to form.

In this work we present a thorough theoretical and experimental study on the performance of the most commonly used catalysts for the synthesis of tetrazoles. The mechanisms and energy barriers involved in the azide–nitrile cycloaddition promoted by each of the catalysts have been assessed through DFT calculations at the M06-2X/6-311+G(d,p) level, including solvent effects. The computational data has been compared with kinetic experiments, all performed under exactly the same conditions and catalyst loadings, therefore allowing a direct comparison of the proficiency of the different additives. In addition, as a result of these investigations, a novel and highly efficient AlCl₃/NMP catalytic system for the preparation of 5-substituted tetrazoles from nitriles and NaN₃ was developed.

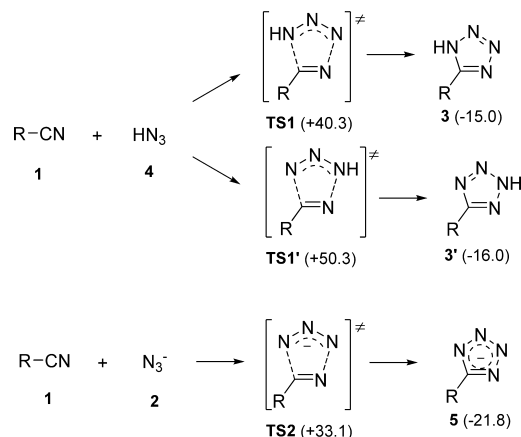
COMPUTATIONAL METHODS

All of the calculations reported in this work were carried out using the Gaussian 09 package.¹⁷ The M06-2X¹⁸ density-functional method in conjunction with the 6-311+G(d,p) basis set was selected for all of the geometry optimizations and frequency analysis. The geometries were optimized including solvation effects. For this purpose, the SMD¹⁹ solvation method was employed. Because *N*-methyl-2-pyrrolidone (NMP) is not internally stored in the Gaussian solvents list, *N,N*-dimethylacetamide (DMA) was selected for all calculations because of their analogous properties. Frequency calculations at 298.15 K on all stationary points were carried out at the same level of theory as the geometry optimizations to ascertain the nature of the stationary points. Ground and transition states were characterized by none and one imaginary frequency, respectively. Benzonitrile and acetonitrile were chosen as model substrates to compute all of the mechanisms and energy barriers. The barriers presented along the manuscript refer to those calculated for the reactions with benzonitrile. Data corresponding to the aliphatic nitrile and discussion of the energetics are collected in the Supporting Information. All of the presented relative energies are free energies at 298.15 K with respect to the reactants.

RESULTS AND DISCUSSION

Uncatalyzed Azide–Nitrile Cycloaddition. In agreement with previous computational investigations with the B3LYP functional,^{14–16} calculations at the M06-2X/6-311+G(d,p) level showed that the direct, uncatalyzed addition of the azide anion **2** and hydrazoic acid **4** to the nitrile group can proceed by a traditional, concerted [3 + 2] Huisgen cycloaddition. For the addition of the neutral HN₃ dipole to the CN group, synchronous transition states were located that give either the 1*H*- or the 2*H*-tetrazole as the product (Scheme 2). An extensive theoretical study on the stability of the two tautomeric forms of various 5-substituted tetrazoles in the gas phase with the DFT method at the B3LYP/6-311++G** level performed in 2001, showed that 2*H*-tetrazoles are more stable

Scheme 2. Formation of 5-Substituted-tetrazoles or the Tetrazolate Anion by a [3 + 2] Huisgen Addition of Hydrazoic Acid or the Azide Anion to Nitriles (R = Ph)



than their 1*H*-tautomers.²⁰ In contrast, our M06-2X calculations, including solvent effects (DMA), predict a slightly higher thermodynamic stability for the 1*H*-tautomer of 5-phenyltetrazole compared to the 2*H*-tautomer by 1.0 kcal mol⁻¹. Calculations in the gas phase at the same level of theory switched their relative stability, with the 2*H*-tautomer more stable by 2.5 kcal mol⁻¹. These data are now in agreement with previous B3LYP calculations,²⁰ and reveal an important solvent effect in the thermodynamic properties of the tetrazole moiety.

The 1,5-approach of HN₃, which results in the 1*H*-tetrazole, is strongly preferred over the 1,3-approach by about 10 kcal mol⁻¹ (Scheme 2). The 1,3-attack of HN₃ occurs in the plane of the aromatic ring and perpendicular to the pπ-orbitals (Figure 1), while the plane of attack for the 1,5-approach is

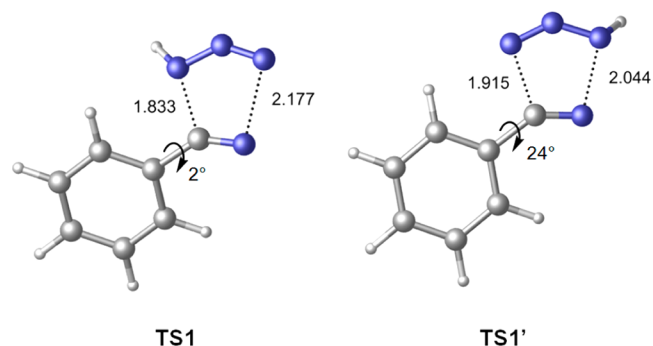


Figure 1. Optimized geometries for the transition states of the [3 + 2] Huisgen cycloaddition of hydrazoic acid with benzonitrile.

twisted out of the plane of the ring by an angle of 24°. The energy barrier for the reaction of the azide anion with benzonitrile is considerably lower than the barrier for the attack of the neutral hydrazoic acid (Scheme 2). The approach of the azide again occurs in the plane of the phenyl ring, but the transition state is noticeably asynchronous with C_{nitrile}–N_{azide} bond distances of 1.63 Å and N_{nitrile}–N_{azide} bond distances of 2.31 Å. The phenyl group of benzonitrile activates the nitrile for tetrazole formation compared to the reaction with acetonitrile and lowers the barrier for the addition of N₃⁻ by ca. 3 kcal mol⁻¹ (see Table S1 in the Supporting Information for further details).

Brønsted Acid Catalyzed Azide–Nitrile Cycloaddition.

The calculations outlined above indicate that tetrazole formation is faster with the electron-rich azide anion as the 1,3-dipolar species, compared to when its protonated counterpart (HN_3) acts as the 1,3-dipole. Experimentally, however, it is found that the reaction is strongly accelerated by Brønsted acids. To prevent the direct handling of the extremely toxic and explosive hydrazoic acid,⁶ tetrazole formation is usually performed with an azide salt (commonly NaN_3) in mildly acidic media. Several Brønsted acid catalysts have been used to accelerate tetrazole synthesis, but the earliest and still most commonly used acids are ammonium salts and acetic acid.^{7,8} Figure 2 depicts the conversions obtained in the reaction of

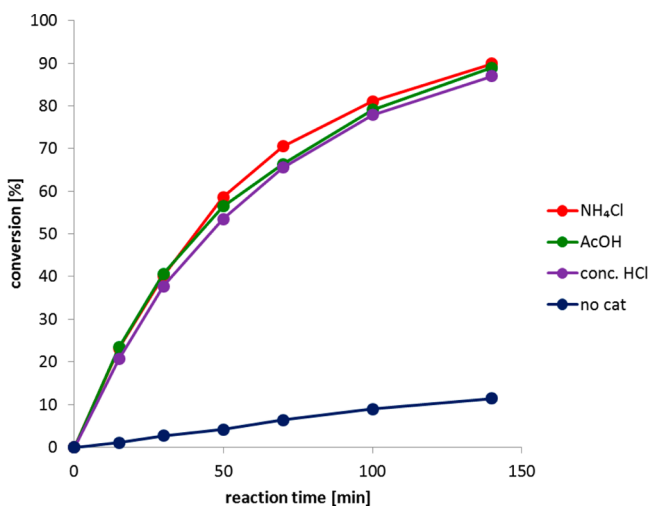


Figure 2. Reaction progress (HPLC conversion at 215 nm) for the cycloaddition of sodium azide with benzonitrile assisted by protic acids. The results for the uncatalyzed process is also shown for comparison. The rate constants have been determined assuming second-order kinetics and reveal a reaction about 20 times faster in the presence of 15 mol % of acid catalyst; $k_{\text{proton}} = 1.007 \times 10^{-2} \text{ L mol}^{-1} \text{ min}^{-1}$; $k_{\text{uncatalyzed}} = 0.04592 \times 10^{-2} \text{ L mol}^{-1} \text{ min}^{-1}$ ($R > 0.99$ in both cases). Conditions: 1 mmol benzonitrile, 2 equiv NaN_3 , and 15 mol % of catalyst, and 1 mL of NMP as solvent heated to a reaction temperature of 160 °C (for reactions with 50% of catalyst, see Figure S1 in the Supporting Information).

benzonitrile with NaN_3 (2 equiv) at 160 °C in the presence of AcOH, NH_4Cl , and conc aqueous HCl in NMP as solvent, compared with the uncatalyzed reaction. Tetrazole formation is significantly accelerated by all of the above-mentioned acids (15 mol %), and all reactions follow a second order rate law with exactly the same rate constant (Figure 2). This indicates that all of these addition reactions proceed by the same mechanism, and apparently the same catalytic species is involved in speeding up the reaction.

Previous mechanistic studies^{14–16} suggested that in the presence of protons the cycloaddition of the azide ion to the nitrile is a stepwise process. The proton activates the nitrile group and increases its reactivity toward the attack of the azide ion. An open imidoyl azide intermediate ($\text{INT}_{1\rightarrow3}$, Scheme 1) is then formed, which subsequently cyclizes in a second step to the 1*H*-tetrazole.^{14–16} Indeed, a hypothetical reaction with the proton of the hydrazoic acid incorporated in a six-membered transition structure (TS3, Figure 3), in which the proton is transferred from hydrazoic acid to the nitrile at the same time as the $\text{C}_{\text{nitrile}}-\text{N}_{\text{azide}}$ bond is formed, has an energy barrier of

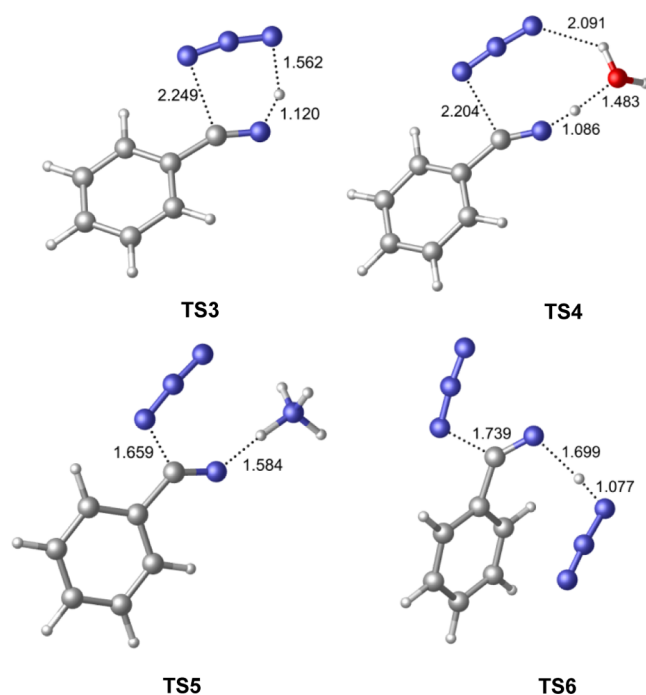


Figure 3. Optimized geometries for the plausible transition states involved in the cycloaddition of azide with nitriles promoted by Brønsted acids.

+37.6 kcal mol⁻¹ with respect to the nitrile and HN_3 . This process leads to the imidoyl azide $\text{INT}_{1\rightarrow3}$ as intermediate, and the energy barrier for this reaction pathway is 12.7 kcal mol⁻¹ lower than for the alternative concerted 1,3-addition of hydrazoic acid to the nitrile and even 2.7 kcal mol⁻¹ lower than the barrier for the 1,5-addition (Scheme 2). However, the barrier is still higher than for the direct cycloaddition of the azide ion to the nitrile, and thus this mechanism does not explain why tetrazole formation is faster under acidic conditions.

Incorporation of a water molecule as a proton shuttle led to the transition structure TS4 in Figure 3, in which the nitrile is receiving a proton from the hydronium ion, and hydrogen bonding between the water and the azide ion stabilizes the structure. The 40.1 kcal mol⁻¹ energy barrier for this reaction, though, is even higher than the barrier for the reaction without water. In contrast, when ammonia is incorporated as mediator (TS5, Figure 3), the energy barrier decreased to 26.8 kcal mol⁻¹ (using as reference the nitrile, hydrazoic acid and ammonia). The barrier is thus almost 11 kcal mol⁻¹ lower than the energy barrier for the unmediated reaction and about 7 kcal mol⁻¹ lower than the barrier for the uncatalyzed [3 + 2] cycloaddition of the azide anion to the nitrile (TS2, Scheme 2). No hydrogen bond interaction between the azide and ammonia could be located for this transition state. The attack of the azide ion to the nitrile carbon occurs in the plane of the phenyl ring of benzonitrile and the $\text{C}_{\text{ph}}-\text{C}-\text{N}$ angle is bent from linearity by approximately 47°. This value contrasts with the 26° and the 29° found for the $\text{C}_{\text{ph}}-\text{C}-\text{N}$ angles for the transition state incorporating water (TS4) and the six-membered ring transition state (TS3), respectively. Together with the much shorter C–N distance for TS5 (1.66 Å) compared to TS3 and TS4 (2.25 and 2.20 Å, respectively), the computed geometries account for a late transition state in the presence of ammonia, which could explain the enhanced reactivity.

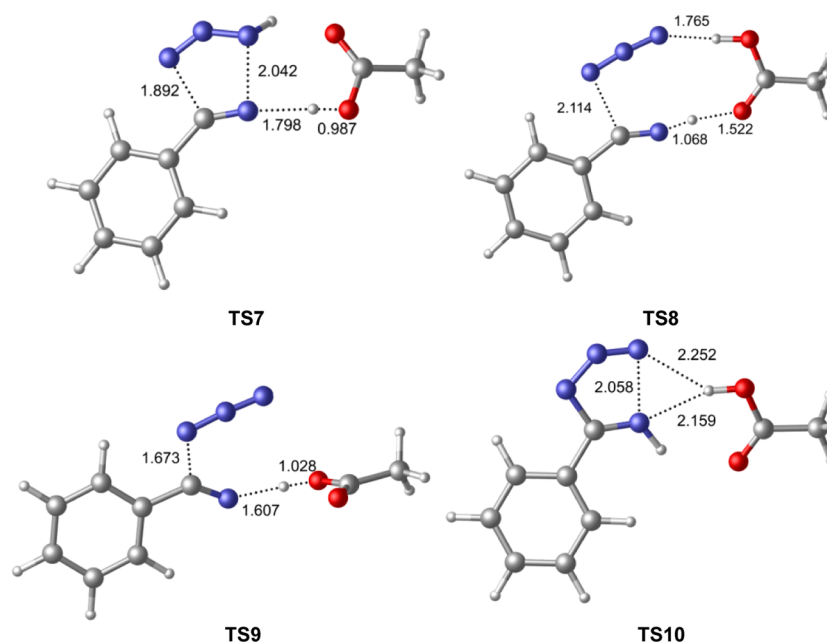


Figure 4. Optimized structures for the plausible transition states involved in the formation of 5-substituted-1H-tetrazoles assisted by acetic acid.

In a similar manner as ammonia, hydrazoic acid itself may assist the formation of the imidoyl azide intermediate $\text{INT}_{1\rightarrow3}$ (TS6, Figure 3). Indeed, activation of benzonitrile with HN_3 and attack of the azide ion gave a very similar energy barrier as that found with NH_3 as the mediator, with a difference in the barriers of only $0.7 \text{ kcal mol}^{-1}$. In this case, the attack of N_3^- occurs slightly outside of the aromatic plane at a dihedral angle of about 142° .

A further commonly used catalyst for the synthesis of tetrazoles is acetic acid.⁸ Several pathways can be envisaged for the tetrazole formation in the presence of this catalyst. A neutral transition state where the nitrile is attached to acetic acid in the transition and the hydrazoic acid adds in a concerted [3 + 2] reaction (TS7, Figure 4) has an energy barrier higher than the barrier of the uncatalyzed concerted cycloaddition of HN_3 ($+46.9 \text{ kcal mol}^{-1}$). In contrast, the acetic acid catalyzed formation of the imidoyl azide intermediate $\text{INT}_{1\rightarrow3}$ from nitrile and hydrazoic acid (TS8, Figure 4) has an energy barrier of $31.2 \text{ kcal mol}^{-1}$. In the course of the $\text{INT}_{1\rightarrow3}$ formation, the nitrile is protonated by the acetic acid while the azide ion, attached to acetic acid by a hydrogen bond, reacts with the electrophilic nitrile carbon. The $\text{C}_{\text{Ph}}-\text{C}-\text{N}$ angle is just slightly bent from linearity in the transition structure by 33° , and the attack of the azide takes place in the plane of the aromatic ring (Figure 4). The alternative reaction with an azide ion instead of HN_3 (TS9, Figure 4) in the presence of acetic acid leads to a transition state with a relative energy of 3 kcal mol^{-1} lower than that found for the neutral process. In this case the $\text{C}_{\text{Ph}}-\text{C}-\text{N}$ angle is bent by 48° in the transition structure, while for the above-described alternative transition structures (TS7 and TS8) a minor deviation from linearity was observed. The shorter C–N distance in TS9 with respect to TS7 and TS8 (Figure 4), along with the angles observed, again suggests a late transition structure with a lower energy barrier.

The open imidoyl azide intermediate $\text{INT}_{1\rightarrow3}$ formed in all of the above-described stepwise addition reactions is rather stable. The reaction of benzonitrile and HN_3 to form $\text{INT}_{1\rightarrow3}$ is endothermic by just $4.6 \text{ kcal mol}^{-1}$. The subsequent ring closing of the $\text{INT}_{1\rightarrow3}$ leading to the tetrazole occurs with an

energy barrier of only $18.2 \text{ kcal mol}^{-1}$ ($22.7 \text{ kcal mol}^{-1}$ with respect to the substrates) and is thus a fast process under the conditions required for tetrazole formation. It should be noted that assistance of a protic species during the ring closing, as exemplified by TS10 (Figure 4), does not enhance efficiency. Thus, in the case of acetic acid, the corresponding barrier in the presence of the protic species (TS10) is $+22.9 \text{ kcal mol}^{-1}$, analogous to the unmediated process.

Comparison of the calculated energy barriers demonstrates that the ammonium salt is the most efficient Brønsted acid for the tetrazole formation, and there is obviously no correlation of the acid strength of the acid catalyst and the rate-accelerating effect. The energy of activation is only $0.7 \text{ kcal mol}^{-1}$ higher for the reaction catalyzed by hydrazoic itself (the pK_a of hydrazoic acid is ~ 4.6 and thus comparable to the pK_a of AcOH), but the other investigated acids, H_3O^+ and AcOH, are significantly less efficient catalysts for the formation of the imidoyl azide. With the acid in catalytic amounts, and in particular in the presence of strong acids, a significant part of the acidic catalyst will be consumed to generate HN_3 , and according to the above calculations, it can be argued that HN_3 is the actual dominant catalytic species for tetrazole syntheses involving Brønsted acids. This conclusion is in perfect agreement with the above-described experimental results (Figure 2), which revealed the same rate constants for all of the Brønsted acid catalyzed reactions.

Lewis Acid Catalyzed Azide–Nitrile Cycloaddition. In 2001 Demko and Sharpless introduced zinc salts as efficient catalysts for the azide–nitrile addition in water as solvent.⁹ This and related protocols have been heavily used since then,⁹ and the mechanism for the zinc-catalyzed reaction, with acetonitrile as the dipolarophile and either N_3^- or methylazide as the 1,3-dipole, was rationalized by B3LYP calculations by Sharpless and Noodleman.¹⁵ According to this study, the zinc salt activates the nitrile moiety by coordination to the nitrogen in a very similar manner as Brønsted acids do, and addition of the azide dipole subsequently furnishes the tetrazole as the product. The addition occurs via a strongly asymmetric transition state, but

an imidoyl azide intermediate as in proton-catalyzed reactions was not located.

We reinvestigated the zinc-catalyzed reaction with the M06-2X functional, including the solvent effects, with the tetrahedral complex **6** as the catalytic species (Figure 5). The complex has

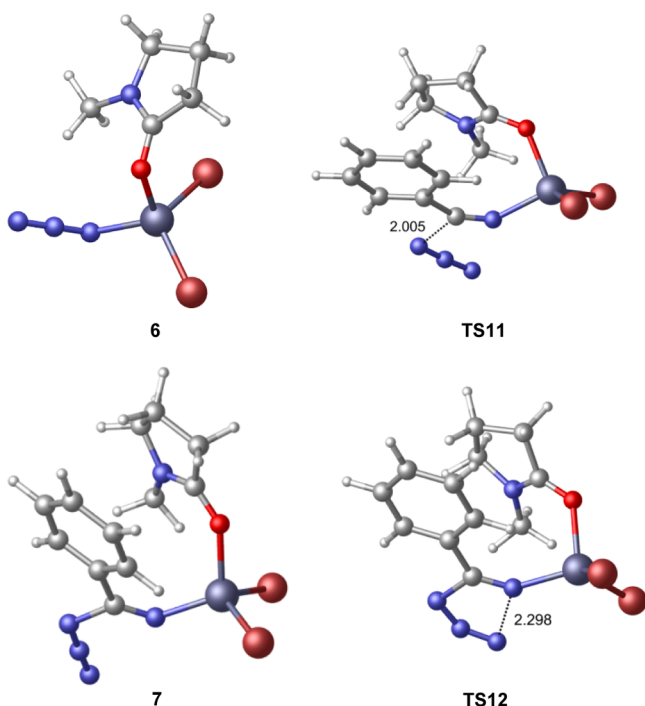


Figure 5. Optimized geometries (M06-2X/6-311+G(d,p)) for the stationary points involved in the reaction of benzonitrile with azide promoted by ZnBr_2 .

an azide, two bromide ions, and a molecule of solvent (NMP) coordinated to the zinc center. Attack of the azide ion to the benzonitrile activated by the zinc complex gave an energy barrier of $25.8 \text{ kcal mol}^{-1}$, leading to a zinc-bonded imidoyl azide **7** (Figure 5) as an open chain intermediate. In contrast to the formation of the imidoyl azide INT_{1-3} in the acid-catalyzed reactions described above, the formation of the **7** is, with a relative energy of $21.4 \text{ kcal mol}^{-1}$, strongly endothermic. On the other hand, the ring-closing process of the **7** to the zinc-bonded tetrazolate via transition structure **TS12** (Figure 5) has an energy barrier of $8.6 \text{ kcal mol}^{-1}$ with respect to the open chain intermediate **7**. Accordingly, the ring closing would actually be the rate-determining step, and the overall barrier is, with $+30.1 \text{ kcal mol}^{-1}$, just 3 kcal mol^{-1} lower than for the uncatalyzed concerted azide–nitrile addition. These results are in good qualitative agreement with experiments performed with benzonitrile and NaN_3 in NMP as solvent (Figure 6). Although the experiments showed a considerable catalytic effect of zinc bromide, the reaction proceeded significantly more slowly than it did with Brønsted acid catalysis.

Aluminum compounds such as $\text{Al}(\text{N}_3)_3$, AlCl_3 , or $\text{Al}(\text{CH}_3)_3$ have also been used as Lewis acid catalysts for the formation of tetrazoles.^{10,15} The proposed mechanism for the reaction of the azide ion with benzonitrile catalyzed by AlCl_3 is analogous to the corresponding mechanism for the ZnBr_2 -catalyzed cycloadditions.²¹ Thus, AlCl_3 coordinates to the nitrile nitrogen and activates the carbon toward the nucleophilic attack of the azide anion. The corresponding transition state **TS13**, with a barrier

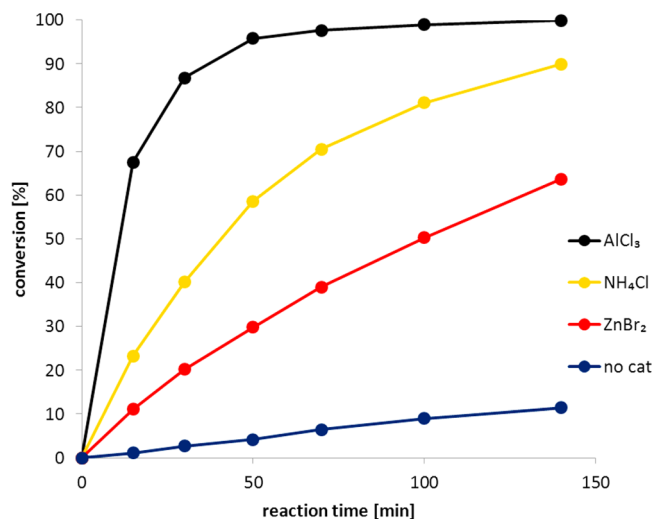


Figure 6. Comparison of the reaction progress (HPLC conversion at 215 nm) for the cycloaddition of sodium azide with benzonitrile assisted by AlCl_3 , NH_4Cl , or ZnBr_2 and the uncatalyzed reaction. The determined rate constants assuming second-order kinetics are $k_{\text{AlCl}_3} = 4.789 \times 10^{-2} \text{ L mol}^{-1} \text{ min}^{-1}$; $k_{\text{NH}_4\text{Cl}} = 1.071 \times 10^{-2} \text{ L mol}^{-1} \text{ min}^{-1}$; $k_{\text{ZnBr}_2} = 0.412 \times 10^{-2} \text{ L mol}^{-1} \text{ min}^{-1}$; $k_{\text{uncatalyzed}} = 0.04592 \times 10^{-2} \text{ L mol}^{-1} \text{ min}^{-1}$ ($R > 0.99$ in all cases). Conditions: 1 mmol benzonitrile, 2 equiv NaN_3 , and 15 mol % of catalyst in 1 mL of NMP as solvent heated to a reaction temperature of $160 \text{ }^\circ\text{C}$ (for reactions with 50% of catalyst, see Figure S1 in the Supporting Information).

of $+28.3 \text{ kcal mol}^{-1}$, leads to an open imidoyl azide structure where the imide nitrogen is coordinated to the aluminum center. The formation of the aluminum-bonded imidoyl azide is rather endothermic ($+14.9 \text{ kcal mol}^{-1}$), but the intermediate is significantly more stable than the zinc-bonded analogue **7**. The subsequent cyclization to the aluminum-bonded tetrazolate occurs faster than the azide–nitrile addition via transition state **TS14** (Figure 7). The calculated energy barrier is $+25.9 \text{ kcal}$

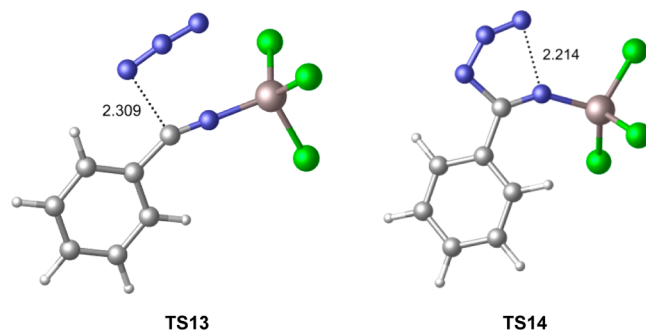


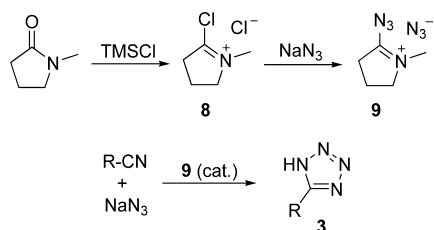
Figure 7. Optimized geometries (M06-2X/6-311+G(d,p)) for the stationary points involved in the reaction of benzonitrile with azide promoted by AlCl_3 .

mol^{-1} . Consequently, the overall barrier is $2.2 \text{ kcal mol}^{-1}$ lower than for the zinc-catalyzed reaction. Furthermore, the energy barrier is $1.5 \text{ kcal mol}^{-1}$ above the barrier of the reaction using the ammonium cation as the catalyst. Experiments indicate, however, that from all catalysts tested during the present study, AlCl_3 is by far the most efficient additive for the reaction of NaN_3 with benzonitrile in NMP as solvent (Figure 6). Obviously, AlCl_3 does not follow the expected mechanism, and other active species are responsible of the rate enhance-

ment as will be described below. The reaction still follows a second-order kinetic for low catalyst loadings, but the rate constant is 1 order of magnitude higher than the rate constant for the ZnBr_2 -catalyzed reaction. Interestingly, increasing the catalyst loading above ca. 25 mol % did not increase the reaction rate further, but rather the rate decreased again. This can be likely ascribed to the formation of $\text{Al}(\text{N}_3)_3$, which is not participating in azide–nitrile additions (see Figure S1 in the Supporting Information for more details).¹⁰

Vilsmeier–Haack-Type Organocatalysts. Our group has recently reported the generation of the Vilsmeier–Haack-type 5-chloro-1-methyl-3,4-dihydro-2*H*-pyrrolium chloride **8** (Scheme 3) during the synthesis of tetrazoles in the presence

Scheme 3. Preparation of Tetrazoles Promoted by the Organocatalyst **9, Generated from NMP and TMSCl**



of catalytic amounts of TMSCl in NMP as solvent.¹⁶ Chloro derivative **8** readily leads to azide structure **9** in the presence of NaN_3 , which displays a remarkably efficient catalytic activity toward tetrazole synthesis. A range of aromatic nitriles could be transformed to the respective tetrazoles with 1.2 equiv of NaN_3 at reaction temperatures of 220 °C and reaction times <20 min.¹⁶ The mechanism of the reaction was explored by DFT calculations at the B3LYP and the M06-2X level.¹⁶ The calculations suggested that, similar to the reaction mechanism of other Lewis acid and proton acid catalysts, the activation of the nitrile is responsible for the rate enhancement. Addition of the azide ion then occurs on the activated nitrile carbon without any energy barrier, and the subsequent ring closing of the imidoyl azide intermediate is the rate-determining step.¹⁶

A comparative reinvestigation of the mechanism at the M06-2X/6-311+G(d,p) level revealed that dihydropyrrolium azide **9** catalyzes the tetrazole formation more efficiently than any other catalyst investigated in the present study. Pyrrolium azide **9** activates the nitrile and a barrier-less attack of the azide ion to the nitrile carbon follows to form the open chain intermediate

10 (Figure 8). The ensuing ring-closing step (**TS15**, Figure 8) of **10** has a barrier of only +25.9 kcal mol⁻¹, which is approximately 1 kcal mol⁻¹ lower than the barrier for the reaction catalyzed by the ammonium cation, the most efficient catalyst previously found in this study. An alternative transition structure **TS16** (Figure 8) was located. In this case, the $\text{C}_{\text{nitrile}}-\text{N}_{\text{azide}}$ bond is formed at the same time as the carbon–azide bond of the catalyst breaks. However, the calculated energy barrier for this concerted azide transfer is rather high (more than 50 kcal mol⁻¹).

In the present work we have now demonstrated that the same Vilsmeier–Haack compound **8**, formed from TMSCl and NMP, is also generated from AlCl_3 and NMP. In contrast to the reaction with TMSCl, which required high temperatures, the formation of **8** from AlCl_3 in NMP occurred readily at room temperature. This was demonstrated by ¹H NMR monitoring of a mixture containing both substances in CDCl_3 (Figure 9)

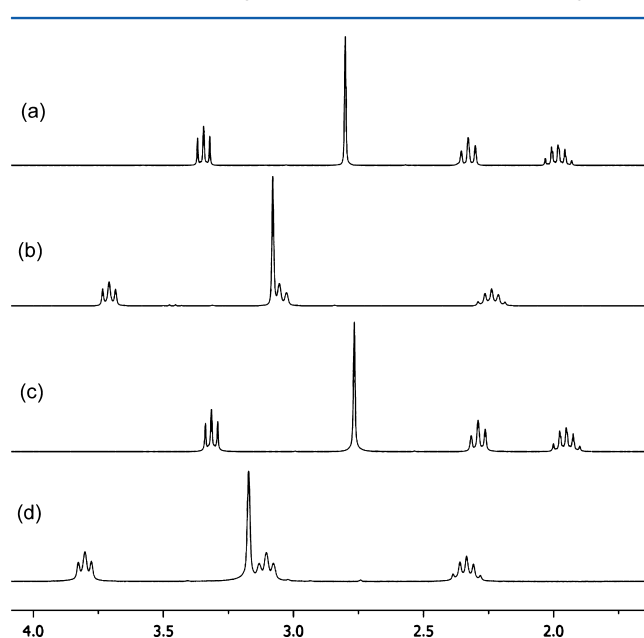


Figure 9. ¹H NMR spectra of solutions in CDCl_3 containing (a) pure NMP, (b) pure pyrrolium chloride **8**, (c) a mixture of TMSCl and NMP, and (d) a mixture of AlCl_3 and NMP. The formation of **8** from AlCl_3 and NMP can be clearly observed (the samples were prepared under argon atmosphere and the spectra recorded immediately upon preparation).

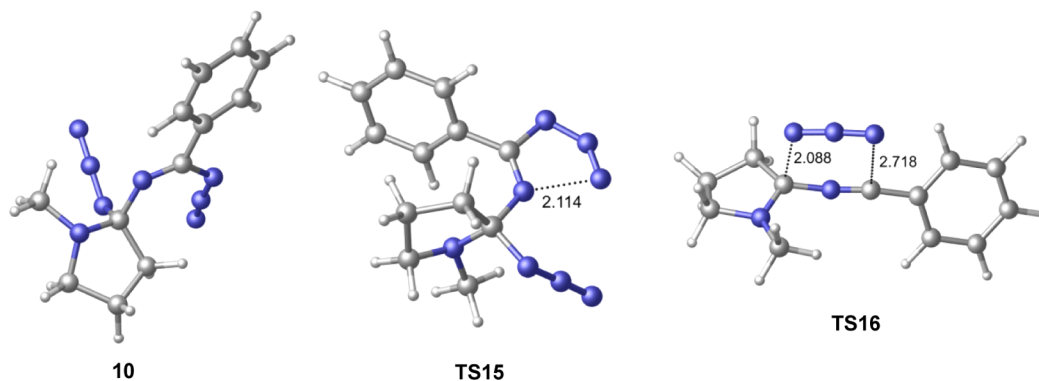
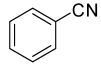
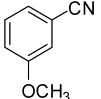
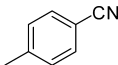
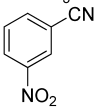
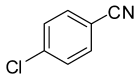
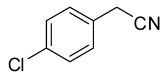
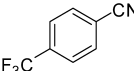
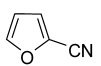


Figure 8. Geometries of the stationary points involved in the tetrazole formation promoted by organocatalyst **9**, optimized at the M06-2X/6-311+G(d,p) level.

Table 1. Preparation of Tetrazoles 3 Promoted by the AlCl₃/NMP System^a

	Substrate	Time (min)	Yield (%) ^b		Substrate	Time (min)	Yield (%) ^b
3a		5	85	3e		7	86
3b		6	97	3f		3	98
3c		4	99	3g		10	82
3d		3	96	3h		3	78

^aReaction conditions: 1 mmol nitrile, 3 mmol NaN₃, 0.15 mmol AlCl₃, and 1.0 mL NMP. Single-mode microwave heating at 200 °C (IR temperature measurement). ^bIsolated yield.

and comparison with the spectra for pure **8**.¹⁶ Importantly, TMSCl showed no reaction with NMP at room temperature (Figure 9).¹⁶ These results indicate that the Vilsmeier–Haack type azido structure **9** (Scheme 3) is the catalytic species in the AlCl₃/NMP system and the facile formation of the dihydropyrrolium cation from AlCl₃ and NMP even at room temperature explains its remarkable catalytic efficiency toward tetrazole synthesis.

AlCl₃ also reacts with DMA at room temperature to produce most likely the corresponding ethaniminium chloride (see Figure S3 in the Supporting Information). Analogous Lewis acidic properties of this species and the dihydropyrrolium cation **8** can be expected. Indeed, tetrazole formation occurred at the same rate with catalytic amounts (15 mol %) of AlCl₃ in DMA and in NMP as solvent (Figure S2 in the Supporting Information). It should be noted that the ethaniminium chloride was not formed from DMA and TMSCl. Correspondingly, tetrazole formation was not appreciably accelerated by TMSCl in DMA as solvent (Figure S2 in the Supporting Information).

Scope of the AlCl₃/NMP System for the Azide–Nitrile Cycloaddition. The AlCl₃/NMP system displayed very high efficiency for the synthesis of 5-phenyl-1H-tetrazole from benzonitrile and NaN₃. To demonstrate the general applicability of this novel reaction system, a series of aromatic nitriles, containing electron-withdrawing and electron-donating groups, were transformed to the corresponding 5-substituted-1H-tetrazoles. Good to excellent yields were obtained for all tested substrates within <10 min reaction time with 15 mol % catalyst loading (Table 1). The required temperature for this protocol (200 °C; for an evaluation of different time/temperature regimes, see Figure S4 in the Supporting Information) is lower than for our previously reported TMSCl/NMP system,¹⁶ and the reaction times are considerably shorter. Isolation of the tetrazole products was simple and only involved dilution with water, precipitation with conc HCl, and subsequent product filtration (**3a–g**) or extraction with ethyl acetate after dilution with water and acidification (**3h**).

CONCLUSIONS

An in-depth computational study at the M06-2X/6-311+G(d,p) level on the catalyzed azide–nitrile cycloaddition has been performed, including several popular additives such as Brønsted acids (AcOH, NH₄Cl, HCl), Lewis acids (zinc and aluminum

salts), and the organocatalyst **9**. In all cases activation of the nitrile group by the catalyst is responsible for the rate enhancement, in a stepwise cycloaddition involving the initial formation of an open-chain imidoyl azide intermediate. Comparative experiments in NMP as solvent carried out under the exact same reaction conditions for all of the catalysts revealed that all Brønsted acids have the same efficiency toward tetrazole formation. Supported by the theoretical calculations, we speculate that in all cases the same species (i.e., HN₃) is involved regardless of the acid strength. Lewis acids such as Zn or Al salts or the organocatalyst **9** perform in a similar manner, activating the nitrile moiety and leading to an open-chain intermediate. All experimental rate constants and theoretical energy barriers obtained in this work are collected in Table 2. The kinetic data qualitatively fit nicely with the computed

Table 2. Calculated Free Energy Barriers at the M06-2X/6-311+G(d,p) Level and Experimental Relative Rate Constants Obtained from the Kinetic Data for All Assessed Catalysts

additive	calcd overall energy barrier (kcal mol ⁻¹)	exptl relative rate constant (× 10 ⁻² L mol ⁻¹ min ⁻¹)
9	25.4	4.789
NH ₄ ⁺	26.8	1.071
HN ₃	27.5	0.976
ZnBr ₂	30.1	0.412
None	33.1	0.0459
AlCl ₃	28.3	<i>a</i>
H ₃ O ⁺	40.2	<i>a</i>
AcOH	28.2	<i>a</i>

^aAlCl₃, HCl and AcOH are not the active species during the azide–nitrile cycloaddition, they lead to **9** (AlCl₃) or HN₃ (HCl and AcOH), which are more efficient catalysts for the tetrazole formation.

energy barriers. Therefore, organocatalyst **9**, formed in situ from AlCl₃ and NMP, is by far the best catalyst evaluated in the present study. Zinc bromide shows a poor efficiency compared to that of **9** and the Brønsted acids, but the reactions still show a significant rate enhancement with respect to the uncatalyzed reaction. In the absence of any catalyst, the azide–nitrile cycloaddition performs rather poorly and thus is difficult to exploit synthetically.²² To the best of our knowledge, this is the first comparative study assessing the reactivity of most of the popular catalytic systems reported for the preparation of

tetrazoles via 1,3-dipolar cycloaddition of azide salts with nitriles. Gratifyingly, theoretical and experimental data show a very good qualitative agreement and reveal the M06-2X functional as a powerful tool for assessing mechanisms involving 1,3-dipolar cycloadditions. In addition, the hitherto unreported AlCl_3/NMP system was shown to catalyze the reaction with unprecedented efficiency. A set of substituted nitriles including electron-withdrawing and electron-donating groups have been transformed in good to excellent yields to the corresponding tetrazoles after reaction times of only 3–10 min at 200 °C.

EXPERIMENTAL SECTION

General Remarks. ^1H NMR spectra were recorded on a 300 MHz instrument. ^{13}C NMR spectra were recorded on the same instrument at 75 MHz. Chemical shifts (δ) are expressed in ppm downfield from TMS as internal standard. The letters s, d, t, q, and m are used to indicate singlet, doublet, triplet, quadruplet, and multiplet, respectively. Analytical HPLC analysis was carried out on a C18 reversed-phase (RP) analytical column (150 mm \times 4.6 mm, particle size 5 mm) at 25 °C using a mobile phase A (water/acetonitrile 90:10 (v/v) + 0.1% TFA) and B (MeCN + 0.1% TFA) at a flow rate of 1.0 mL min^{-1} . The following gradient was applied: linear increase from 30% solution B to 100% B in 8 min, hold at 100% solution B for 2 min. Melting points were determined on a standard melting point apparatus in open capillaries. All anhydrous solvents (stored over molecular sieves) and chemicals were obtained from standard commercial vendors and were used without any further purification.

Procedure for the Kinetic Experiments (Figures 2 and 6). To a solution of the corresponding catalyst (0.15 mmol) in anhydrous NMP (1.0 mL) were added NaN_3 (130 mg, 2.0 mmol) and the corresponding nitrile (1.0 mmol). The reaction mixture was placed in a sealed Pyrex screw cap reaction vial and heated on a hot plate equipped with a silicon carbide heating block with a 6 \times 4 deep well matrix preheated at 160 °C.²³ The reaction progress was monitored by HPLC (215 nm) by injecting samples of approximately 2 μL diluted in acetonitrile.

General Procedure for the Synthesis of 5-Substituted-1H-tetrazoles 5 (Table 1). To a solution of anhydrous AlCl_3 (19.9 mg, 0.15 mmol) in anhydrous NMP (1.0 mL) were added NaN_3 (195 mg, 3.0 mmol) and the corresponding nitrile (1.0 mmol). The reaction mixture was stirred for 1 min and was subsequently irradiated in a single-mode microwave instrument (Biotage Initiator 2.5) at 200 °C (IR temperature measurement) for 3–10 min (see Table 1). Workup A: The reaction mixture was poured into 10 mL of H_2O . The pH of the solution was adjusted to \sim pH 1 with concentrated HCl (Caution: gas evolution). The mixture was cooled in an ice-bath, and the precipitate was collected by filtration and washed thoroughly with cold 1 N HCl to furnish the desired tetrazole. Workup B: The reaction mixture was poured into 10 mL of saturated NaHCO_3 and extracted three times with 20 mL of CHCl_3 . The aqueous phase was carefully acidified with concentrated HCl to \sim pH 1 (Caution: gas evolution) and extracted three times with 20 mL of EtOAc. The combined organic phases were dried over magnesium sulfate and concentrated in vacuo to obtain the pure tetrazole products, identical in all respects to sample previously prepared in our laboratories using a similar method.¹⁶ The purity of all synthesized compounds (>98%) was established by either HPLC at 215 nm or ^1H NMR spectroscopy.

Caution: Hydrazoic acid and its salts are highly poisonous compounds, and hydrazoic acid itself and many of its heavy metal salts explode easily without obvious reasons. Proper protective measures (proper shielding and an additional safety screen in the fume hood, safety glasses or a face shield, leather coat, leather or Kevlar gloves) should be used when undertaking work involving NaN_3/HN_3 .

5-Phenyltetrazole (3a). Yield 124 mg (85%, workup A); mp 217–218 °C, lit.^{9b} mp 215–215 °C with decomp; ^1H NMR (300 MHz, $\text{DMSO}-d_6$) δ 7.59–7.61 (m, 3H), 8.03–8.06 (m, 2H).

5-(4'-Tolyl)tetrazole (3b). Yield 155 mg (57%, workup A); mp 251–252 °C, lit.^{11b} mp 246–248 °C with decomp; ^1H NMR (300 MHz, $\text{DMSO}-d_6$) δ 7.93 (d, J = 8.0 Hz, 2H), 7.41 (d, J = 8.0 Hz, 2H), 2.38 (s, 3H).

5-(4'-Chlorophenyl)tetrazole (3c). Yield 180 mg (99%, workup A); mp 252–254 °C with decomp, lit.^{11b} mp 252–254 °C; ^1H NMR (300 MHz, $\text{DMSO}-d_6$) δ 8.05 (d, J = 8.4 Hz, 2H), 7.69 (d, J = 8.4 Hz, 2H).

5-(4'-(Trifluoromethyl)phenyl)tetrazole (3d). Yield 206 mg (96%, workup A); mp 222–223 °C with decomp, lit.^{11b} mp 221–222 °C; ^1H NMR (300 MHz, $\text{DMSO}-d_6$) δ 8.25 (d, J = 8.1 Hz, 2H), 7.98 (dd, J = 8.1 Hz, 2H).

5-(3'-Methoxyphenyl)tetrazole (3e). Yield 152 mg (86%, workup A); mp 158–160 °C, lit.²⁴ mp 156–157 °C; ^1H NMR (300 MHz, $\text{DMSO}-d_6$) δ 7.58–7.63 (m, 2H), 7.51 (t, J = 8.0 Hz, 1H), 7.16 (dd, J = 2.4 and 8.1 Hz, 1H), 3.85 (s, 3H).

5-(3'-Nitrophenyl)tetrazole (3f). Yield 187 mg (98%, workup A); mp 118–120 °C with decomp, lit.²⁵ mp 145–146 °C; ^1H NMR (300 MHz, $\text{DMSO}-d_6$) δ 8.82 (s, 1H), 8.40–8.47 (m, 2H), 7.90 (t, J = 8.1 Hz, 1H).

5-((4'-Chlorophenyl)methyl)tetrazole (3g). Yield 160 mg (82%, workup A); mp 160–162 °C, lit.²⁶ mp 164 °C; ^1H NMR (300 MHz, $\text{DMSO}-d_6$) δ 7.41 (d, J = 8.4 Hz, 2H), 7.30 (d, J = 8.4 Hz, 2H), 4.30 (s, 2H).

5-(2'-Furyl)tetrazole (3h). Yield 106 mg (78%, workup B); mp 201–203 °C, lit.²⁴ mp 204–205 °C; ^1H NMR (300 MHz, $\text{DMSO}-d_6$) δ 8.06 (m, 1H, CH), 7.29 (d, J = 3.6 Hz, 1H, CH), 6.79–6.81 (m, 1H, CH).

ASSOCIATED CONTENT

Supporting Information

Supplementary tables and figures, complete ref 17, Cartesian coordinates, energy, and imaginary frequency (transition states) for all of the calculated stationary points. This material is available free of charge via the Internet at <http://pubs.acs.org>.

AUTHOR INFORMATION

Corresponding Author

*E-mail: oliver.kappe@uni-graz.at.

Notes

The authors declare no competing financial interest.

ACKNOWLEDGMENTS

This work was supported by a grant from the Christian Doppler Research Society (CDG). D.C. thanks the Spanish Ministerio de Ciencia e Innovación for a fellowship and the Research, Technological Innovation, and Supercomputing Center of Extremadura (CénitS) for their support in the use of LUSITANIA computer resources.

REFERENCES

- (1) Butler, R. N. In *Comprehensive Heterocyclic Chemistry*; Katritzky, A. R., Rees, C. W., Scriven, E. F. V., Eds.; Pergamon: Oxford, U.K., 1996; Vol. 4.
- (2) (a) Herr, R. J. *Bioorg. Med. Chem.* **2002**, *10*, 3379–3393. (b) Myzchnik, L. V.; Hrabalek, A.; Koldobskii, G. I. *Chem. Heterocycl. Compd.* **2007**, *43*, 1–9. (c) Roh, J.; Vávrová, K.; Hrabálek, A. *Eur. J. Org. Chem.* **2012**, 6101–6118. (d) Koldobskii, G. I. *Russ. J. Org. Chem.* **2006**, *42*, 487–504.
- (3) Hantzsch, A.; Vagt, A. *Liebigs Ann. Chem.* **1901**, *314*, 339–369.
- (4) Dimroth, O.; Fester, G. *Ber. Dtsch. Chem. Ges.* **1910**, *43*, 2219–2223.
- (5) Mihina, J. S.; Herbst, R. M. *J. Org. Chem.* **1950**, *15*, 1082–1092.
- (6) For a discussion of safety aspects in handling HN_3 , see: (a) Kopach, M. E.; Murray, M. M.; Braden, T. M.; Kobierski, M. E.; Williams, O. L. *Org. Process Res. Dev.* **2009**, *13*, 152–160. (b) *Organic*

Azides: Syntheses and Applications; Bräse, S., Banert, K., Eds.; Wiley-VCH, Weinheim, 2010.

(7) (a) Finnegan, W. G.; Henry, R. A.; Lofquist, R. *J. Am. Chem. Soc.* **1958**, *80*, 3908–3911. (b) Alterman, M.; Hallberg, A. *J. Org. Chem.* **2000**, *65*, 7984–7989. (c) Roh, J.; Artamonova, T. V.; Vávrová, K.; Koldobskii, G. I.; Hrabálek, A. *Synthesis* **2009**, 2175–2178.

(8) (a) Gutmann, B.; Roduit, J.-P.; Roberge, D.; Kappe, C. O. *Angew. Chem., Int. Ed.* **2010**, *49*, 7101–7105. (b) Schmidt, B.; Meid, D.; Kieser, D. *Tetrahedron* **2007**, *63*, 492–496. (c) Herbst, R. M.; Wilson, K. R. *J. Org. Chem.* **1957**, *22*, 1142–1145. (d) McManus, J. M.; Herbst, R. M. *J. Org. Chem.* **1959**, *24*, 1044–1046.

(9) For zinc-catalyzed reactions, see: (a) Demko, Z. P.; Sharpless, K. B. *J. Org. Chem.* **2001**, *66*, 7945–7950. (b) Demko, Z. P.; Sharpless, K. B. *Org. Lett.* **2001**, *3*, 4091–4094. (c) Shie, J. J.; Fang, J. M. *J. Org. Chem.* **2007**, *72*, 3141–3144. (d) Myznikova, L. V.; Roh, J.; Artamonova, T. V.; Hrabalek, A.; Koldobskii, G. I. *Russ. J. Org. Chem.* **2007**, *43*, 765–767.

(10) For aluminum-catalyzed reactions, see: (a) Behringer, H.; Kohl, K. *Chem. Ber.* **1956**, *89*, 2648–2653. (b) Matthews, D. P.; Green, J. E.; Shuker, A. J. *J. Comb. Chem.* **2000**, *2*, 19–23. (c) Huff, B. E.; Staszak, M. A. *Tetrahedron Lett.* **1993**, *34*, 8011–8014. (d) McManus, J. M.; Herbst, R. M. *J. Org. Chem.* **1959**, *24*, 1464–1467. (e) Arnold, C.; Thatcher, D. N. *J. Org. Chem.* **1969**, *34*, 1141–1142. (f) Aureggi, V.; Sedelmeier, G. *Angew. Chem., Int. Ed.* **2007**, *46*, 8440–8444.

(11) Other additives: (a) Venkateshwarlu, G.; Premalatha, A.; Rajanna, K. C.; Saiprakash, P. K. *Synth. Commun.* **2009**, *39*, 4479–4485. (b) Bonnamour, J.; Bolm, C. *Chem.—Eur. J.* **2009**, *15*, 4543–4545.

(12) (a) Kantam, M. L.; Kumar, K. B. S.; Raja, K. P. *J. Mol. Catal. A* **2006**, *247*, 186–188. (b) Kantam, M. L.; Balasubrahmanyam, V.; Kumar, K. B. S. *Synth. Commun.* **2006**, *36*, 1809–1814. (c) Nasrollahzadeh, M.; Bayat, Y.; Habibi, D.; Moshae, S. *Tetrahedron Lett.* **2009**, *50*, 4435–4438. (d) He, J.; Li, B.; Chen, F.; Xu, Z.; Yin, G. *J. Mol. Catal. A* **2009**, *304*, 135–138. (e) Das, B.; Reddy, C. R.; Kumar, D. N.; Krishnaiah, M.; Narender, R. *Synlett* **2010**, 391–394.

(13) (a) Kantam, M. L.; Kumar, K. B. S.; Sridhar, C. *Adv. Synth. Catal.* **2005**, *347*, 1212. (b) Lang, L.; Li, B.; Liu, W.; Jiang, L.; Xu, Z.; Yin, G. *Chem. Commun.* **2010**, *46*, 448–450.

(14) Himo, F.; Demko, Z. P.; Noodleman, L.; Sharpless, K. B. *J. Am. Chem. Soc.* **2002**, *124*, 12210–12216.

(15) Himo, F.; Demko, Z. P.; Noodleman, L.; Sharpless, K. B. *J. Am. Chem. Soc.* **2003**, *125*, 9983–9987.

(16) Cantillo, D.; Gutmann, B.; Kappe, C. O. *J. Am. Chem. Soc.* **2011**, *133*, 4465–4475.

(17) *Gaussian 09*, Revision A.1; Frisch, M. J. et al.; Gaussian, Inc.: Wallingford, CT, 2009.

(18) Zhao, Y.; Truhlar, D. G. *Theor. Chem. Acc.* **2008**, *120*, 215–241.

(19) Marenich, A. V.; Cramer, C. J.; Truhlar, D. G. *J. Phys. Chem. B* **2009**, *113*, 6378–6396.

(20) Sadlej-Sosnowska, N. *J. Org. Chem.* **2001**, *66*, 8737–8743.

(21) The theoretical calculations were performed using AlCl₃ as Lewis acid although we are aware that in the presence of an excess of NaN₃, Al(N₃)₃ will be readily formed. Analogous results are expected using Al(N₃)₃, which however would unnecessarily complicate the calculations.

(22) For a recent claim of an uncatalyzed azide–nitrile cycloaddition, see: Palde, P. P.; Jamison, T. F. *Angew. Chem., Int. Ed.* **2011**, *50*, 3525–3528.

(23) Kappe, C. O.; Damm, M. *Mol. Diversity* **2012**, *16*, 5–25.

(24) Amantini, D.; Belaggia, R.; Fringuelli, F.; Pizzo, F.; Vaccaro, L. *J. Org. Chem.* **2004**, *69*, 2896–2898.

(25) Jursic, B. S.; LeBlanc, B. W. *J. Heterocycl. Chem.* **1998**, *35*, 405–408.

(26) Wehman, T. C.; Popov, A. I. *J. Phys. Chem.* **1966**, *70*, 3688–3693.